Austin Publishing Group

Hydrogen Generation from Steam Methane Reforming on the Nanostructured Ni-Re Alloy Surface of the Total Metallic Honeycomb Catalysts

Wang L[1,2]*

[1]National Institute for Materials Science, Tsukuba, Japan.

[2]National Institute of Advanced Industrial Science and Technology, Tsukuba, Japan.

***corresponding author:** **Linsheng wang,** National Institute for Materials Science, Tsukuba, Ibaraki 305-0047, Japan., Email: linsheng_wang@yahoo.com & wang.linsheng@aist.go.jp

Published Date: July 10, 2021

Abstract

The nanostructured Ni and Ni-Re alloy active species are successfully fabricated on the surface of the total metallic Ni honeycomb substrate and the porous Ni metal as the novel catalyst system for hydrogen generation from steam methane reforming. The bimetallic Ni-Re nanoalloy active species on the surface of the metallic Ni honeycomb substrate or porous Ni metal substrate exhibit the remarkably enhanced activity for steam methane reforming to generate hydrogen especially at lower reaction temperatures. The total metallic catalysts with excellent electric and heat conductivity and almost zero bed pressure loss are expected to be used for the innovation industrial processes.

Keywords: Hydrogen generation; Methane steam reforming; Ammonia; Temperature.

Introduction

Hydrogen is an energy carrier and large quantities of H_2 are needed in the petroleum and chemical industries and semiconductor industry including the processing ("upgrading") of fossil fuels and the production of ammonia. About 53 million metric tons hydrogen were consumed worldwide every year. There are no natural hydrogen deposits and for this reason the production of hydrogen plays a key role in modern society. The majority of hydrogen (about 95%) is produced from fossil fuels by steam reforming or partial oxidation of methane and coal gasification with only a small quantity by other routes such as biomass gasification or electrolysis of water. For this process at high temperatures steam (H_2O) reacts with methane (CH_4) in an endothermic reaction to yield syngas. In a second stage, additional hydrogen is generated through the lower-temperature exothermic water gas shift reaction:

$$CO + H_2O \rightarrow CO_2 + H_2$$

A highly active and sulfur-tolerant bimetallic Ni–Re catalyst system for hydrogen generation from gasoline fuels by steam reforming and oxidative steam reforming has been reported in our previous studies [1-4]. The promotional effect of Re on the activity and stability of Ni/Al_2O_3 catalyst was found and a green process for gasoline reforming to produce hydrogen while inhibiting formation of methane on Ni–Re-based catalysts at lower reaction temperatures was developed [5-7]. The high gasoline conversion of 100% with the low concentration of methane product is maintained very well during 700 h of operation for steam reforming of desulfurized gasoline fuel at the lower reaction temperature. The high activity and sulfur tolerance of $Ni\text{-}Re/Al_2O_3$ is due to the alloying of Ni with Re to form the bimetallic Ni-Re alloy nanoparticles. Recently the metallic Ni honeycomb catalyst have been reported and the Ni honeycomb catalyst exhibited catalytic activity for Methane Steam Reforming (MSR) under low steam-to-carbon ratio and gas hourly space velocity conditions [8,9]. Metallic honeycomb catalysts have several advantages compared with conventional pelleted catalysts such as: low pressure drop per

Citation: Wang L, (2021). Hydrogen Generation from Steam Methane Reforming on the Nanostructured Ni-Re Alloy Surface of the Total Metallic Honeycomb Catalysts. Importance & Applications of Nanotechnology, Austin Publishing Group. Vol. 1, Chapter 1, pp. 1-7.

catalyst volume, fast heat and mass transport [10-14]. These advantages are important for their applications in hydrogen production systems, although improving of the activity of the Ni honeycomb catalyst especially at lower temperatures is still a challenge because the performance was unsatisfactorily low under higher SV. It is necessary to improve this issue in a wide temperature range. In the present presentation, nanostructured Ni and Ni-Re active species are fabricated on the surface of the total metallic Ni honeycomb and the porous Ni metal as the novel catalyst system for hydrogen generation from steam methane reforming.

Experimental

Ni honeycomb preparation and catalytic reaction

The pure Ni honeycomb substrate (diameter 6mm, height 5mm) was assembled by combining 30μm thick flat and wave-shaped pure Ni foils. Ni nanoparticles were supported on the surface of Ni honeycomb substrate to obtain the Ni/Ni honeycomb sample by impregnating the Ni honeycomb substrate in aqueous solution of $Ni(NO_3)_2$ at room temperature. Ni-Re nanoparticles were supported on Ni honeycomb substrate to obtain the Ni-Re/Ni honeycomb sample by impregnating the Ni/Ni honeycomb in aqueous solution of NH_4ReO_4 at room temperature. After impregnation the samples were dried, calcined, and reduced with H_2. The catalytic tests were carried out in the temperature range of 673-1173K at atmospheric pressure for steam reforming of methane in a fixed bed continuous-flow quartz reactor. Before the steam reforming reaction, the catalysts were reduced by H_2/N2 at 703 K for 1 h.

Catalyst characterization

The nanostructured honeycomb catalysts were characterized by XRD, SEM-EDAX etc. The Brunauer-Emmett-Teller (BET) specific surface area of the honeycomb before and after the reactions was measured with Kr adsorption using a surface area analyzer (Micromeritics, ASAP 2020). The surface morphology was analyzed using a Scanning Electron Microscope (SEM; JEOL, JSM-7000F) coupled with an X-ray Energy Dispersive Spectroscopy (EDS) system.

Results and discussion

Activity improvement of Ni honeycomb by deposition of Ni nanoparticles on its surface

The activities of the Ni honeycomb substrate and the Ni honeycomb coated with Ni nanoparticles (Ni/Ni honeycomb) for steam methane reforming at a SV of 1200h^{-1} and a reaction temperature of 973K are compared in Figure 1. We can see from Figure 1 that the conversion of methane on the Ni honeycomb substrate is only about 10% under the given reaction conditions. However, the conversion of methane on the Ni substrate coated with Ni nanoparticles (Ni/Ni honeycomb) is more than 80% under the same reaction conditions. The much higher activity of the Ni/Ni honeycomb than that of the pure Ni honeycomb substrate is contributed to the Ni nanoparticles coated on the Ni honeycomb substrate. Therefor coating of Ni nanoparticles on the surface of Ni honeycomb substrate is effective to improve the catalytic activity of the pure Ni honeycomb catalyst at lower reaction temperature and higher SV.

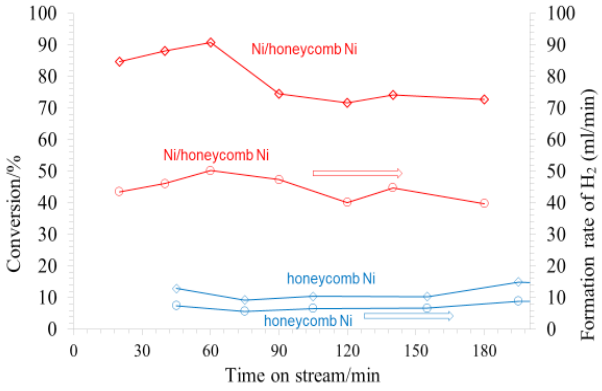

Figure 1: Activity improvement of honeycomb Ni by deposition of Ni nanoparticles on the surface. Reaction conditions: T=973K; SV=1200h-1; Mole ratio of $CH_4/H_2O/N_2$=3/5/1.

It is clear in Figure 1 that the activity of the Ni honeycomb substrate is low for steam methane reforming at the given reaction temperatures and the activity of the Ni honeycomb catalysts with deposited Ni nanoparticles on the surface (Ni/honeycomb Ni) is evidently improved. The methane conversion on the Ni/Ni-honeycomb at the reaction temperature of 973K and SV of 1200h^{-1} and the mole ratio of $CH_4/H_2O/N_2$ of 3/5/1 is about 80%, which is about 5 time higher than that on the Ni honeycomb substrate.

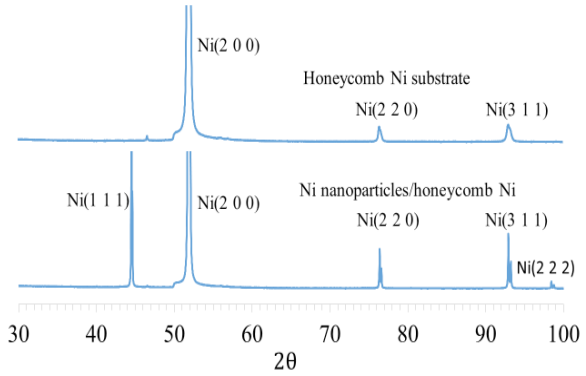

Figure 2: XRD patterns of the Ni nanoparticles deposited on the honeycomb Ni.

Figure 2 shows the XRD patterns of the Ni honeycomb substrate and the Ni honeycomb deposited with Ni nanoparticles on the surface. It is clear in Figure 2 that 3 XRD peaks of the Ni (200) peak at the 2theta angel of 52 degree, the Ni (220) peak at the 2theta angel of 77degree and the Ni (311) peak at the 2theta angel of 93 degree are appeared on the Ni honeycomb substrate. The Ni (111) peak at the 2theta angel of 44.5 degree is also appeared after Ni nanoparticles is deposited on the surface of the honeycomb Ni, which is not appeared on the Ni honeycomb substrate. Therefore, the Ni (111) peak at the 2theta angel of about 44.5 degree is assigned to the Ni nanoparticles deposited on the Ni honeycomb substrate. The increased activity of Ni/honeycomb Ni is ascribed to the Ni nanoparticle on the surface of the Ni honeycomb.

Effect of alloying of Ni with Re to form Ni-Re alloy nanoparticles on the surface of Ni honeycomb

Figure 3 shows the conversions for steam methane reforming on Ni/Ni-honeycomb and Ni-Re/Ni honeycomb catalysts at different reaction temperatures and a SV of 1200h^{-1} and mole ratio of $CH_4/H_2O/N_2$ of 3/5/1.

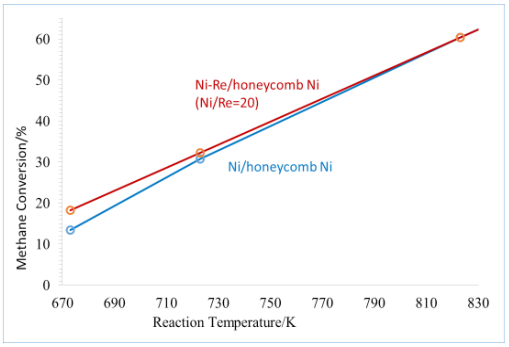

Figure 3: Low temperature activity enhancement by alloying of Ni with Re on the surface of honeycomb Ni at SV of 1200h^{-1} and $CH_4/H_2O/N_2$ mole ratio of 3/5/1.

We can see from Figure 3 that the activity of Ni-Re/Ni-honeycomb catalyst is evidently higher than that of Ni/Ni honeycomb catalyst at the lower reaction temperatures of 673K and 723 K. This indicates that the bimetallic Ni-Re alloy nanoparticles formed by alloying of Ni with Re is more active that the monometallic Ni nanoparticles supported on the surface of Ni honeycomb Ni substrate for steam methane reforming to generate hydrogen. The activities of the two catalysts become close with increasing reaction temperature as shown in Figure 3. This indicates that the steam methane reforming reaction becomes thermochemical equilibrium with increasing the reaction temperature.

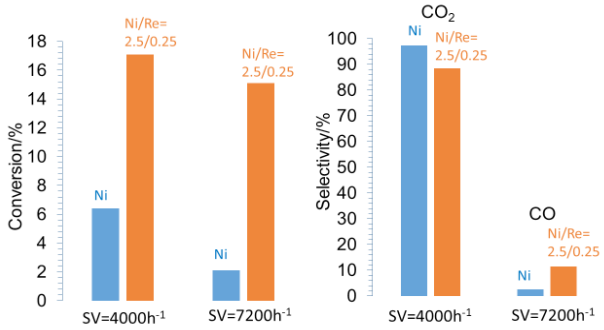

Figure 4: Effect of surface alloying of Ni with Re on activity and selectivity of Ni (2.5wt.%) /Ni honeycomb catalyst for steam methane reforming at 723K.

Figure 4 compares the activity of Ni (2.5wt.%)-Re (0.25wt.%)/Ni honeycomb and Ni (2.5wt.%)/Ni honeycomb for steam methane reforming at a low reaction temperature of 723K and the high SV of 4000h^{-1} and 7200h^{-1}.

We can see from Figure 4 that the activity enhancement of the Ni/Ni honeycomb catalyst for steam methane reforming by surface alloying of Ni with Re to form Ni-Re alloy nanoparticles become more remarkably at the increasing Space Velocity (SV). The methane conversion on Ni (2.5wt.%)-Re (0.25wt.%)/Ni honeycomb catalyst is about 2 times higher than that on Ni (2.5 wt.%)/Ni honeycomb catalyst at a SV of 4000h^{-1} and the methane conversion on Ni (2.5wt.%)-Re (0.25wt.%)/Ni honeycomb catalyst is about 7 times higher than that on Ni (2.5 wt.%)/Ni honeycomb catalyst at a SV of 7200h^{-1} as shown in Figure 4.

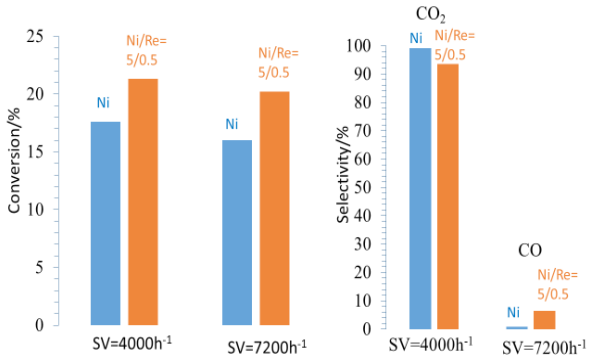

Figure 5: Effect of surface alloying of Ni with Re on activity and selectivity of Ni (5wt.%) /Ni honeycomb catalyst for steam methane reforming at 723K.

Figure 5 compares the activity of Ni (5wt.%)-Re (0.5wt.%)/Ni honeycomb and Ni (5wt.%)/Ni honeycomb for steam methane reforming at a low reaction temperature of 723K and high SV of 4000h^{-1} and 7200h^{-1}. We can see from Figure 5 that the activity enhancement of the Ni/Ni honeycomb catalyst for steam methane reforming by surface alloying of Ni with Re to form Ni-Re alloy nanoparticles become more evidently at the increasing Space Velocity (SV). The methane conversion on Ni (5wt.%)-Re (0.5wt.%)/Ni honeycomb catalyst and Ni (5wt.%)/Ni honeycomb catalysts is about 22% and 18% respectively at a SV of 4000h^{-1} and the methane conversion on Ni (5wt.%)-Re (0.5wt.%)/Ni honeycomb catalyst and Ni (5wt.%)/Ni honeycomb catalysts is about 22% and 16% respectively at a higher SV of 7200h^{-1} as shown in Figure 5.

The CO_2 selectivity on Ni/Ni honeycomb catalysts is higher than that on Ni-Re/Ni honeycomb catalysts as shown in Figure 4 and 5. The activity of Ni (5wt.%)-Re (5wt.%)/Ni honeycomb, Ni (5wt.%)-Re (10wt.%)/Ni honeycomb and Ni (5wt.%)/Ni honeycomb catalysts for steam methane reforming at different reaction temperatures and a high SV of 20000h^{-1} are compared in Figure 6.

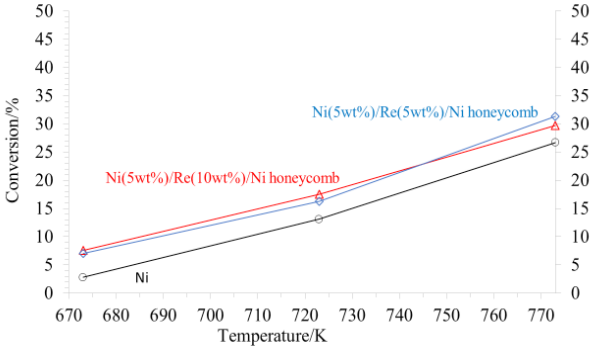

Figure 6: Effect of surface alloying of Ni with Re on the activity for hydrogen generation by methane steam reforming at a high SV of 20000h^{-1} and the $CH_4/H_2O/N_2$ mole ratio of 3/5/9.

We can see from Figure 6 that the activity of Ni (5wt.%)-Re (5wt.%)/Ni honeycomb and Ni (5wt.%)-Re (10wt.%)/Ni are much higher than that of the Ni/Ni honeycomb catalyst for steam methane reforming at the high space velocity (SV) of 20000 h^{-1} and a wide rage of reaction temperatures. However,the activity of Ni (5wt.%)-Re (10wt.%)/Ni honeycomb is a little higher than that of Ni (5wt.%)-Re (5wt.%)/Ni honeycomb as shown in Figure 6. We also use porous Ni with average pore size of 450μm as substrate to prepare the Ni(10wt%)/porous-Ni and Ni(10wt%)-Re(1wt%)/porous-Ni catalysts for steam methane reforming. The activities of the Ni(10wt%)/porous Ni and Ni(10wt%)-Re(1wt%)/porous Ni catalysts for steam methane reforming at a wide range of reaction temperature from 673K to 1173K are compared in Figure 7. We can see from Figure 7 that the Ni(10wt%)-Re(1wt%)/porous Ni catalyst exhibits the evident activity at 673K and methane conversion increases with increasing reaction temperature from 673K to 1173K. However, the starting reaction temperature

for catalysing steam methane reforming on Ni (10wt%)/porous Ni is about 1023K. Therefor the activity Ni/porous Ni for steam methane reforming is remarkably enhanced by surface alloying of Ni with Re to form Ni-Re alloy nanoparticles on the porous Ni substrate as shown in Figure 7.

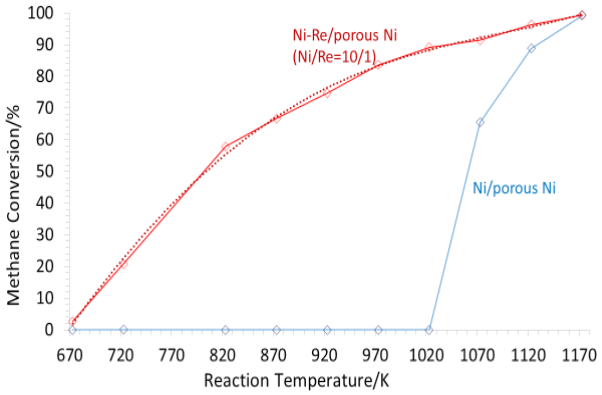

Figure 7: Activity comparison of the Ni(10wt%)/porous Ni and Ni(10wt%)-Re(1wt%)/porous Ni catalysts for steam methane reforming at a wide range of reaction temperature from 673-1173K with $CH_4/H_2O/N_2$ mole ratio of 3/5/9 and SV of 6580h^{-1}.

The structures of the bimetallic Ni-Re alloy nanoparticles and the monometallic Ni nanoparticles are examined by XRD. Figure 8 and 9 shows the XRD patterns of Ni (5wt.%)-Re (2wt.%)/Ni honeycomb, Ni (5wt.%)-Re (1wt.%)/Ni honeycomb, Ni (5wt.%)-Re (0.5wt.%)/Ni honeycomb and Ni (5wt.%)/Ni honeycomb samples. We can see from Figure 8 that the Ni (111) peak at 2theta angel of 44.5 degree become wider after alloying of Ni nanoparticles with Re to form Ni-Re alloy nanoparticles. This indicates that the surface alloying of Ni with Re improving the dispersion of the Ni nanoparticles on the Ni honeycomb. In order to observe the change of Ni (111) peak more clearly after surface alloying of Ni with Re, we enlarge the XRD patterns from 2 theta angel range from 40 to 50 degree as shown in Figure 9. We can clearly see from Figure 8 that a new peak near the Ni (111) peak is appeared on Ni-Re/Ni honeycomb samples. However, this new peak is not appeared on Ni/Ni honeycomb sample. Therefor this new XRD peak is assigned to the Ni-Re alloy nanoparticles formed by surface alloying of Ni with Re.

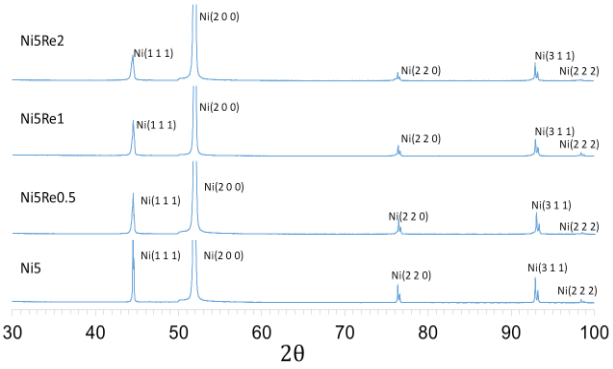

Figure 8: XRD patterns of Ni (5wt.%)-Re (2wt.%)/Ni honeycomb, Ni (5wt.%)-Re (1wt.%)/Ni honeycomb, Ni (5wt.%)-Re (0.5wt.%)/Ni honeycomb and Ni (5wt.%)/Ni honeycomb samples.

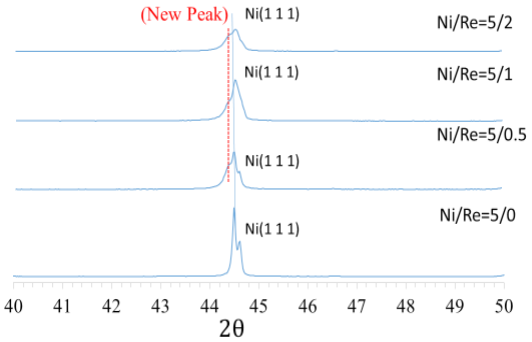

Figure 9: XRD patterns of Ni (5wt.%)-Re (2wt.%)/Ni honeycomb, Ni (5wt.%)-Re (1wt.%)/Ni honeycomb, Ni (5wt.%)-Re (0.5wt.%)/Ni honeycomb and Ni (5wt.%)/Ni honeycomb samples at the 2 theta angel of 40-50.

The structures of the bimetallic Ni-Re alloy nanoparticles and the monometallic Ni nanoparticles are examined by XRD. Figure 8 and 9 shows the XRD patterns of Ni (5wt.%)-Re (2wt.%)/Ni honeycomb, Ni (5wt.%)-Re (1wt.%)/Ni honeycomb, Ni (5wt.%)-Re (0.5wt.%)/Ni honeycomb and Ni (5wt.%)/Ni honeycomb samples. We can see Figure 8 that the Ni (111) peak at 2theta angel of 44.5 degree become wider after alloying of Ni nanoparticles with Re to form Ni-Re alloy nanoparticles. This indicates that the surface alloying of Ni with Re improving the dispersion of the Ni nanoparticles on the Ni honeycomb. In order to observe the change of Ni (111) peak more clearly after surface alloying of Ni with Re, we enlarge the XRD patterns from 2 theta angel range from 40 to 50 degree as shown in Figure 9. We can clearly see from Figure 8 that a new peak near the Ni (111) peak is appeared on Ni-Re/Ni honeycomb samples. However, this new peak is not appeared on Ni/Ni honeycomb sample. Therefor this new XRD peak is assigned to the Ni-Re alloy nanoparticles formed by surface alloying of Ni with Re.

The monometallic Ni nanoparticles are synthesized by reduction of their oxide precursors of NiO and the bimetallic Ni-Re alloy nanoparticles are synthesized by their precursors of NiO·ReOx. The precursors of the bimetallic Ni-Re alloy nanoparticles and the monometallic Ni nanoparticles are observed by SEM and their images are shown in Figure 10.

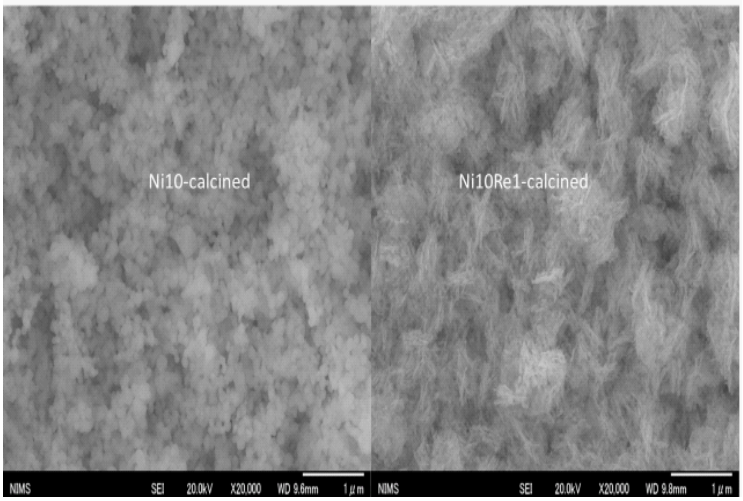

Figure 10: SEM images of precursors for synthesis of the bimetallic Ni-Re alloy nanoparticles and the monometallic Ni nanoparticles on Ni honeycomb substrate.

We can find from Figure 10 that the SEM images of the precursors for bimetallic Ni-Re alloy nanoparticles are look quite different from the SEM images of the precursors for monometallic Ni nanoparticles. The SEM images of the precursors for bimetallic Ni-Re alloy nanoparticles look like the nanofibers. The SEM images of the precursors for monometallic Ni nanoparticles are nanoparticles.

Conclusion

Two types of total metallic catalysts of Ni honeycomb and porous Ni which are deposited with bimetallic Ni-Re alloy nanoparticles with excellent electric and heat conductivity and almost zero bed pressure loss are successfully fabricated. The surface alloying effect of Ni with Re lead to the appearing of new XRD peak which is assigned to the synthesized bimetallic Ni-Re nanoparticles. The bimetallic Ni-Re alloy nanoparticles deposited on Ni honeycomb substrate or porous Ni substrate exhibit the remarkably enhanced activity for steam methane reforming to generate hydrogen especially at lower reaction temperatures by comparison with the monometallic Ni nanoparticles deposited on the Ni honeycomb substrate or porous Ni substrate.

References

1. Wang L, Murata K, Inaba M. Development of novel highly active and sulphur-tolerant catalysts for steam reforming of liquid hydrocarbons to produce hydrogen. Appl Catal A: Gen. 2004; 257: 43-47.

2. Wang L, Murata K, Inaba M. Control of the product ratio of $CO_2/(CO+CO_2)$ and inhibition of catalyst deactivation for steam reforming of gasoline to produce hydrogen. Appl Catal B: Environ. 2004; 48: 243-248.

3. Murata K, Wang L, Saito M, Inaba M, Takahara I, Mimura N. Energy Fuels. 2004; 18: 122-126.

4. Wang L, Murata K, Inaba M. Conversion of Liquid Hydrocarbons into H_2 and CO_2 by Integration of Reforming and the Water-Gas Shift Reaction on Highly Active Multifunctional Catalysts. Ind Eng Chem Res. 2004; 43: 3228-3232.

5. Wang L, Murata K, Inaba M. Steam reforming of gasoline promoted by partial oxidation reaction on novel bimetallic Ni-based catalysts to generate hydrogen for fuel cell-powered automobile applications. J Power Sources. 2005; 145: 707-711.

6. Wang L, Murata K, Matsumura Y, Inaba M. Lower-Temperature Catalytic Performance of Bimetallic Ni–Re/Al_2O_3 Catalyst for Gasoline Reforming to Produce Hydrogen with the Inhibition of Methane Formation. Energy Fuels. 2006; 20: 1377-1381.

7. Wang L, Murata M, Inaba M. Highly efficient conversion of gasoline into hydrogen on Al_2O_3-supported Ni-based catalysts: Catalyst stability enhancement by modification with W. Applied Catalysis A: General. 2009; 358: 264-268.

8. Fukuhara C, Yamamoto K, Makiyama Y, Kawasaki W, Watanabe R. High Performance of a Structured Ni-Based Catalyst for Autothermal Dry Reforming of Methane. Appl Catal A: Gen. 2015; 492: 190-200.

9. Hiramitsu Y, Demura M, Xu Y, Yoshida M, Hirano T. Catalytic properties of pure Ni honeycomb catalysts for methane steam reforming. Appl Catal A: Gen. 2015; 507: 162-168.

10. Hiramitsu Y, Demura M, Xu Y, Yoshida M, Hirano T. Catalytic properties of pure Ni honeycomb catalysts for methane steam reforming. Appl Catal A. 2015; 507: 162.

11. Flytzani-Stephanopoulos M, Voecks GE, Charng T. Modelling of heat transfer in non-adiabatic monolithic reactors. Chem Eng Sci. 1986; 43: 1203-1212.

12. Farrauto RJ, Liu Y, Ruettinger W, Ilinich O, Shore L, et al. Catal Rev. 2007; 49: 141-196.

13. Xu Y, Harimoto T, Wang L, Hirano T, Kunieda H, et al. Chemical Engineering & Processing: Process Intensification. 2018; 129: 63-70.

14. Hiramitsu Y, Demura M, Xu Y, Yoshida M, Hirano T. Catalytic properties of pure Ni honeycomb catalysts for methane steam reforming. Appl Catal A. 2015; 507: 162.